Petroleum & Coal
ISSN 1337-7027

Available online at www.vurup.sk/petroleum-coal
Petroleum & Coal 56(3) 231-248, 2014

HYDROGEN AND GASOLINE PRODUCTION THROUGH THE COUPLING OF FISCHER–TROPSCH SYNTHESIS AND CYCLOHEXANE DEHYDROGENATION IN A THERMALLY COUPLED MEMBRANE REACTOR

H. Nouryzadeh, D. Iranshahi

Chemical Engineering Department, Amirkabir University of Technology, Tehran 15875, Iran

Received April 10, 2014, Accepted June 16, 2014

Abstract

The present study investigates hydrogen and gasoline production in a heat exchanger reactor through the process intensification concept. The mentioned reactor is composed of two concentric tubular fixed bed reactors. The endothermic dehydrogenation of cyclohexane is considered to take place in the shell side of Fischer–Tropsch pilot plant of research institute of petroleum industry, instead of currently used water, to enhance low sulfur gasoline and pure hydrogen by using membrane technology. The co–current mode is considered and the simulation results are compared with the corresponded conventional Fischer–Tropsch reactor data at the identical process conditions. This novel reactor configuration increases the selectivity/yield of gasoline compared with the conventional reactor. Also hydrogen can be produced as a valuable fuel. The performance of the reactor is investigated for different operating variables. However, the operability of the reactor needs to be proven experimentally and be tested over a range of parameters under practical operating conditions.

Keywords: Hydrogen production; Indirect coupling; Fischer–Tropsch synthesis; Dehydrogenation of cyclohexane.

1. Introduction

Nowadays a great deal has been concerned on the absence of naturally oil reservoirs near the future. At the same time, extensive reserves of natural gas exist in many regions that lack sufficient petroleum. The growing demand for clean liquid fuels (i.e., zero sulphur) has triggered an international effort to develop methods for production and commercialization of these valuable energy resources [1-2]. So the production of hydrocarbons from syngas through Fischer–Tropsch synthesis (FTS) has attracted much attention in both catalysis and chemical engineering fields during the last century. These high quality products (due to absence of toxic sulfur and low aromatic content) as fuel have been proven to be environmentally friendly compared with those from conventional crude oil route [3]. Compared with the crude-oil-derived diesel, FTS fuel has been shown to reduce the emissions of CO, nitrogen oxides, hydrocarbons, and other particulates [4].

On the other hand, future energy systems must provide a secure, more sustainable, suitable, climate and environmentally friendly energy supply. Hydrogen has been nominated as a renewable and alternative energy. It is an efficient energy carrier. It offers cost effective solutions to reduce greenhouse gases, improve air quality, diversify energy supply and reduce noise. It is supposed to be used as heat and power sources in power plants, such as gas turbines [5–8].

1.1. Hydrogen

There are several techniques to produce hydrogen such as coal gasification, reforming of fossil fuels and hydrocarbons. Production of hydrogen from methanol and ethanol has been investigated by many authors. Electrolysis of water is the other option for pure hydrogen production in small case production [9–12]. Currently, 80–85% of the world's total hydrogen production is derived via steam methane reforming (SMR) of natural gas [13]. In such cases, however, the same amount of carbon dioxide is released during the production of hydrogen

which forms by direct combustion of fuels. This method produces toxic and corrosive components such as CO, CO_2 and H_2S in addition to trace amounts of ammonia [14]. Dehydrogenation is an attractive alternative for hydrogen production because it has essentially zero CO_2 impact giving a positive environmental contribution [15]. In this way, Itoh *et al*. [16] used cyclohexane as a chemical hydrogen carrier. The main advantage of using cyclohexane as a carrier component rather than others is from the following points of view: its higher hydrogen content (e.g., 7.1 wt.% of cyclohexane) is very attractive compared to metal hydrides (at most 3 wt. %), The dehydrogenated products, benzene and toluene, can be reversibly hydrogenated and reused and those are all liquids at ordinary temperatures. On the other hand no CO_2 emission in the dehydrogenation process will be rated highly in terms of environmental issues, whereas the steam reforming process of methanol produces not only hydrogen but also CO_2.

1.2. Membranes (Pd-Ag membranes)

In the recent years membranes are used extensively in the applicable researches as a function to enhance the products yield/selectivity and thermodynamically shift the reactions toward products. The first large-scale commercial application of membrane gas separation was the separation of hydrogen from nitrogen, methane and argon in an ammonia plant [17]. Rahimpour *et al*. [18-25] used membrane in the fixed bed reactors of methanol, naphtha reforming and FT synthesis to improve the yields of reactions. Also they proposed novel configurations of reactors for methanol and FT process, by inserting a perm–selective membrane into dual–type and fluidized bed reactors in order to control the doze of hydrogen along the reactor. Tosti *et al*. [26] have described different configurations of palladium membrane reactors used for separating ultra pure hydrogen. Lin *et al*. [27] found that membrane reactors for methanol steam reforming at 300–400℃ can be feasible for hydrogen production. Nair *et al.* [28] recently carried out a comprehensive study on the synthesis and permeation characterization of a series of Pd and Pd–Ag membranes. They measured the permeation flux of H_2 over a range of temperature, pressure and time on stream. Palladium combines excellent hydrogen transport and selectivity properties, resistance to high temperature conditions and corrosion. These properties would make palladium membranes very attractive for use with petrochemical gases [15].

1.3. Fischer–Tropsch synthesis

F–T synthesis is either low temperature (LTFT) process or high temperature (HTFT) process depending on the product required. High temperature process is mainly used for the production of gasoline and linear olefins [29]. Ahmadi Marvast [30] modeled a water–cooled fixed bed F–T reactor in two dimensions, used the intrinsic rates were developed at RIPI (Research Institute of Petroleum Industry) to produce gasoline from synthesis gas. Fuels produced from the F–T process are of high quality due to a very low aromaticity and absence of sulfur. The octane number of F–T gasoline is lower than the gasoline obtained from crude oil processing, since the F–T gasoline mainly consists of n–paraffin [30]. Various reactor types such as fixed bed, fluidized bed and slurry have been considered during the F–T process development [22-23]. Fixed bed F–T synthesis reactors are conventional and large scale commercial gasoline production.

1.4. Coupled Reactors

Process intensification (PI), known as the strategy of miniaturizing process plants, is a novel design approach which can reduce equipment size by several orders of magnitude leading to substantial saving in capital cost, improvement of intrinsic safety and reducing environment impact [31]. In recent years, an extension of their applications for gas pulsation, swirling fluidized bed, immersed tube arrays, internally circulating fluidized bed and electrical fluidized bed have been parametrically studied [32]. Coupling of endothermic and exothermic reactions have been attempted as an intense plant through the PI category. The reactors for coupling exothermic and endothermic reactions have received wide attention due to their potential to provide compact hydrogen generation systems [33].

There are several ways for coupling exothermic and endothermic reactions that can be broadly classified into recuperative coupling (counter–current heat exchanger reactor, co–current heat exchanger reactor), regenerative coupling (reverse–flow reactor) and direct coupling (directly coupled adiabatic reactor). A schematic of various reactor configurations

for coupling exothermic and endothermic reactions was presented by Ramaswamy *et al*. [34]. Hunter and McGuire [35] were the pioneers who suggested coupling of endothermic with exothermic reaction by means of indirect heat transfer. They considered heat exchangers where catalytic combustion or other highly exothermic reaction was used as a heat source for an endothermic reaction. Choudhary *et al*. [36] coupled exothermic and endothermic reactions in oxidative conversion of ethane to ethylene over alkaline earth metal promoted La_2O_3 catalysis in presence of steam and limited O_2 at different temperatures. Itoh and Wu [16, 38] investigated an adiabatic type of palladium membrane reactor for coupling endothermic and exothermic reactions. On one side of membrane, dehydrogenation of cyclohexane took place in the catalyst packed layer, and on the membrane surface of the other side hydrogen permeated react in–situ with oxygen. Khademi *et al*. [15, 38, 39] coupled methanol synthesis reaction with cyclohexane dehydrogenation in a novel thermally coupled membrane reactor. Also they investigated the optimal conditions for this configuration and compared with corresponded prediction for a conventional methanol fixed bed reactor. Elnashaie *et al*. [40] considered the specific system of simultaneous catalytic dehydrogenation of ethylbenzene and hydrogenation of benzene coupled through the hydrogen selective membranes. Abo–Ghander *et al*. [41] studied the catalytic dehydrogenation of ethylbenzene to styrene, coupled with the catalytic hydrogenation of nitrobenzene to aniline in a simulated integrated reactor, formed of two fixed beds separated by a hydrogen–selective membrane.

The subject of previous works on GTL (Fischer-Tropsch) by Rahimpour *et al.* was not in the category of coupled reactors [25]. They just replaced the conventional fixed bed reactor of Fischer-Tropsch process by two fixed and fluidized bed membrane reactors to increase the production rate of gasoline. The use of membrane in the second reactor controls the hydrogen content of reaction side. In other words, previously only one process (Fischer-Tropsch) had been focused while in our new manuscript simultaneously Fischer-Tropsch synthesis and dehydrogenation of cyclohexane are focused for higher performance.

2. Process description

In industrial fixed bed F–T reactors, multi tubular reactors cooled by pressurized boiling water are often used. Fig. 1 shows the scheme of the conventional reactor (CR) for F–T synthesis. Table 1 represents the characteristics of the CR developed by RIPI [23]. Another way of controlling the reactor temperature is the use of an endothermic reaction in the shell side of CR.

Table1 Fischer – Tropsch pilot plant characteristics.

Parameter	Value
Tube dimension [mm]	$Ø38.1^a \times 3^b \times 12000^c$
Molar ratio of H_2/CO in feed	0.96
Feed temperature [K]	565
Reactor pressure [kPa]	1700
Cooling temperature [K]	566.2
Catalyst sizes [mm]	$Ø2.51^a \times 5.2^c$
Catalyst density [kgm^{-3}]	1290
Bulk density [kgm^{-3}]	730
Number of tubes	1
Tube length [m]	12
GHSV [h^{-1}]	235
Bed voidage	0.488
Feed molar flow rate [g mol s^{-1}]	0.0335

a: Diameter, b: Wall thickness, c: Length

The endothermic reaction can play the role of a heat sink and properly control the exothermic side temperature. When the exothermic reaction is fast, more heat will generate and transfer to the endothermic side. Consequently, the reaction rate for the endothermic side increases and more heat is consumed. In one word, the cooling medium (endothermic side) can properly adjust its temperature according to the exothermic side. Fig. 2(a) and (b) show the schematic of proposed configuration in co–current mode of operation. By inserting a Pd-Ag perm–selective

membrane, hydrogen can selectively remove through the second side and pure hydrogen is produced in the third side.

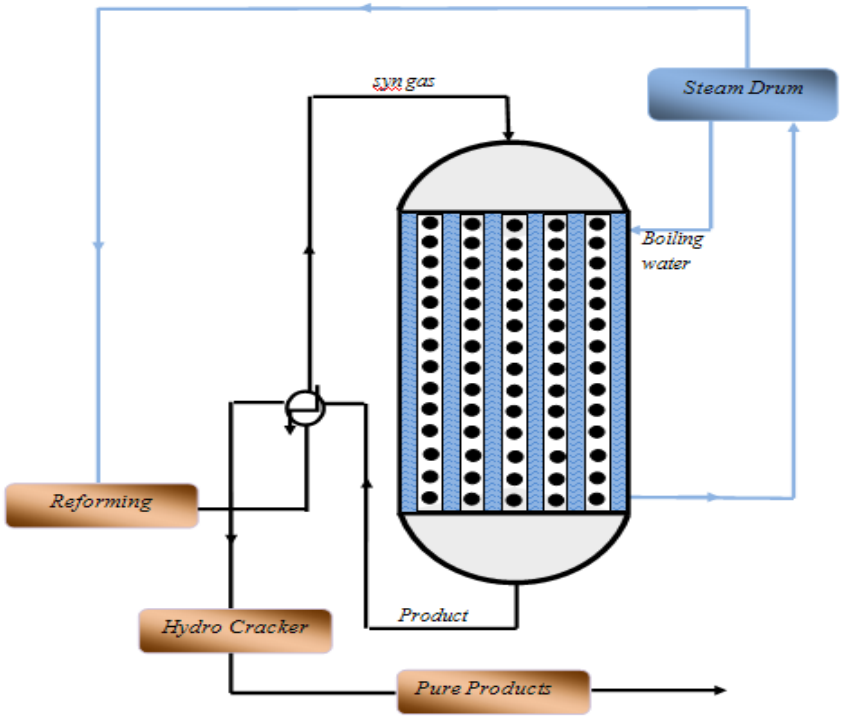

Fig. 1 Schematic diagram for conventional fixed bed Fischer–Tropsch reactor

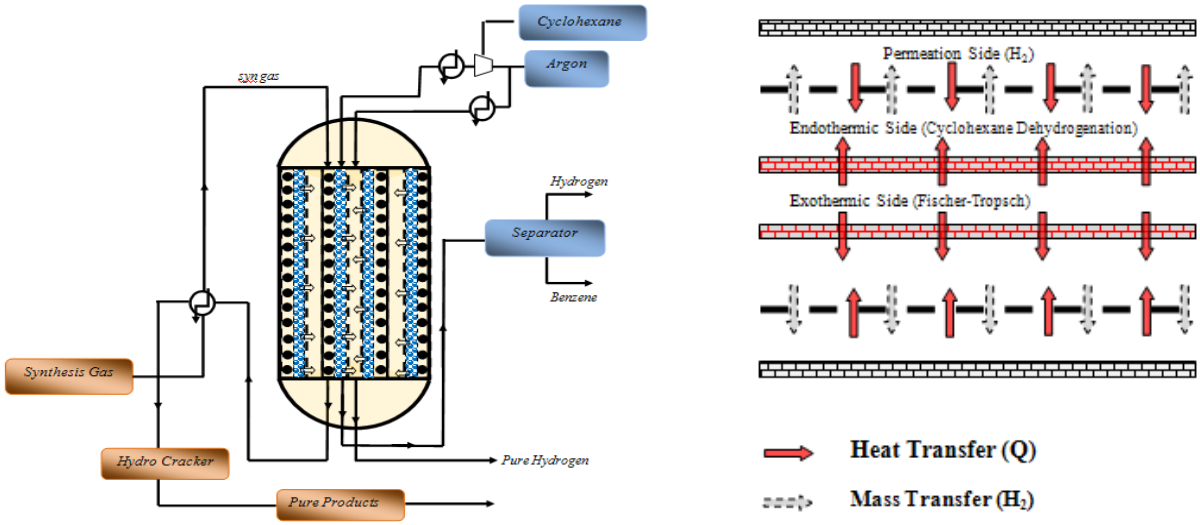

Fig. 2 Schematic diagram for thermally coupled membrane reactor configuration (a) and (b).

This new work combines the beneficial aspects of previous works briefly through the mathematical modeling as follow:

- Supplying the required heat of endothermic side (dehydrogenation of cyclohexane) via Fischer-Tropsch reaction.
- Production of three valuable products, benzene, hydrogen and gasoline, simultaneously.
- Reduction the size and volume of plants, instead of using separate Fischer-Tropsch and dehydrogenation units.
- Enduration of catalyst life time.

Mathematical modeling is an excellent tool to provide a good initial sense of what can be achieved in the coupled reactors.

3. Reaction scheme and kinetics

3.1. Fischer–Tropsch synthesis

The F–T process involves a variety of competing chemical reactions, which leads to a series of desirable and undesirable products. The most important reactions are, those result in the formation of alkanes. Generally, the F–T process operates in the temperature range of 150–300°C. Increasing the pressure leads to higher conversion rates and also favors formation of long–chained alkanes that they are both desirable. Typical pressures are in the range of one to several tens of atmospheres. Chemically, even higher pressures would be favorable, but the benefits may not justify the additional costs of high–pressure equipment [42]. The F–T components include H_2, CO, CO_2, H_2O, CH_4, C_2H_6, C_3H_8, n–C_4H_{10}, i–C_4H_{10} and C_5^+ (gasoline). The following reactions are considered as dominate F–T reactions:

$$CO + 3H_2 \xrightarrow{R_1} CH_4 + H_2O \quad (1)$$

$$2CO + 4H_2 \xrightarrow{R_2} C_2H_4 + 2H_2O \quad (2)$$

$$2CO + 5H_2 \xrightarrow{R_3} C_2H_6 + 2H_2O \quad (3)$$

$$3CO + 7H_2 \xrightarrow{R_4} C_3H_8 + 3H_2O \quad (4)$$

$$4CO + 9H_2 \xrightarrow{R_5} n - C_4H_{10} + 4H_2O \quad (5)$$

$$4CO + 9H_2 \xrightarrow{R_6} i - C_4H_{10} + 4H_2O \quad (6)$$

$$6.05CO + 12.23H_2 \xrightarrow{R_7} C_{6.05}H_{12.36}(C_{5^+}) + 6.05H_2O \quad (7)$$

$$CO + H_2O \xleftrightarrow{R_8} CO_2 + H_2 \quad (8)$$

$$r_i = 0.278.k_i.\exp(-E_i/RT).P_{CO}^m.P_{H_2}^n \qquad mol/kg_{cat}.s \quad (9)$$

The developed reaction rate equation by RIPI is as follow and the kinetic parameters are given in Table 2:

Table 2 Kinetic parameter data for Fischer–Tropsch synthesis

Reaction No.	m	n	k_i	E_i
1	-1.0889	1.5662	142583.8	83423.9
2	0.7622	0.0728	51.556	65018
3	-0.5645	1.3155	24.717	49782
4	0.4051	0.6635	0.4632	34885.5
5	0.4728	1.1389	0.00474	27728.9
6	0.8204	0.5026	0.00832	25730.1
7	0.5850	0.5982	0.02316	23564.3
8	0.5742	0.710	410.667	58826.3

3.2. Dehydrogenation of cyclohexane

The reaction scheme for the dehydrogenation of cyclohexane to benzene is as follows:

$$C_6H_{12} \leftrightarrow C_6H_6 + 3H_2 \qquad \Delta H_{298} = +206.2kJ/mol \quad (10)$$

The following rate of reaction is used for cyclohexane [43]:

$$r_c = \frac{-k(K_P P_C / P_{H_2}^3 - P_B)}{1+(K_B K_P P_C / P_{H_2}^3)} \quad (11)$$

where k, K_B, and K_P are respectively the reaction rate constant, the adsorption equilibrium constant for benzene and the reaction equilibrium constant that are tabulated in Table 3. P_i is the partial pressure of component *i* in Pa. The reaction temperature is in the range of 423–523 K and the total pressure in the reactor is maintained at 101.3 kPa [44].

Table 3 The reaction rate constant, the adsorption equilibrium constant, and the reaction equilibrium constant for dehydrogenation of cyclohexane reaction

$k = A\exp(B/T)$	*A*	*B*
k	0.221	-4270
K_B	2.03×10^{-10}	6270
K_P	4.89×10^{35}	3190

4. Mathematical modeling

The following assumptions are considered during the modeling of heat exchanger reactor (coupled reactors):

- One–dimensional heterogeneous model (reactions take place in the catalyst particles).
- Steady state conditions and no time dependency in temperature and concentration along the reactor length in each side.
- Plug flow pattern is considered in reactor and tube side.
- Axial diffusion of heat and mass are neglected compared to the convection.
- Total molar flow rate is considered to be constant along the reactor length.
- Intra-pellet heat and mass diffusion in catalyst pellet is neglected.
- Bed porosity in axial and radial directions is constant.
- Gas mixtures considered to be ideal.
- Heat loss is neglected.

4.1. Heat and mass balance equations

A differential element is considered along the axial direction inside the reactor. The mass and energy balances are written for solid and fluid phases in all sides and hydrogen permeation through the membrane. The results are summarized in Table 4. In equations (12) and (13) η is effectiveness factor of k^{th} reaction in j^{th} side of reactor (effectiveness factor is the ratio of the reaction rate observed to the real rate of reaction), which is obtained from a dusty gas model calculations [45]. In Equations (14) and (15), β is equal to 1 for the endothermic side and 0 for the exothermic side. The positive sign in equation (15), is used for the exothermic side and the negative sign for the endothermic side. In this equation the forth term is related to heat transfer by hydrogen permeation. In equations (16) and (17), β is equal to 1 for hydrogen component and 0 for the sweeping gas. j_{H_2} is the hydrogen permeation rate for Pd-Ag membrane. P_{H_2} is hydrogen partial pressure in Pa. D_o and D_i stand for the outer and inner diameters of the Pd-Ag layer. The pre exponential factor P_0 above 200 °C is reported as $6.33\times10^{-8}\, molm^{-2}s^{-1}Pa^{\frac{-1}{2}}$ and the activation energy E_p is 15.7 $kJmol^{-1}$ [25].

Table 4 Mass and energy balances for solid and fluid phases in all sides, hydrogen permeation in Pd-Ag membrane, and boundary conditions.

Definitions	Equations	
Solid phase	$a_v c_j k_{gi,j}(y^g_{i,j} - y^s_{i,j}) + \eta r_{i,j}\rho_b = 0$	(12)
	$a_v h_f (T^g_j - T^s_j) + \rho_b \sum_{i-1}^{N} \eta r_{i,j}(-\Delta H_{f,i}) = 0$	(13)
Fluid phase	$-\frac{F_j}{A_c}\frac{dy^g_{i,j}}{dz} + a_v c_j k_{gi,j}(y^s_{i,j} - y^g_{i,j}) - \beta\frac{J_{H_2}}{A_c} = 0$	(14)
	$-\frac{F_j}{A_c}C^g_{pj}\frac{dT^g_j}{dz} + a_v h_f (T^s_j - T^g_j) \pm \frac{\pi D_i}{A_c}U(T^g_2 - T^g_1)$	(15)
	$-\beta\frac{j_{H_2}}{A_c}\int_{T_2}^{T_3} C_p dT - \beta\frac{\pi D_i}{A_c}U_{2-3}(T^g_2 - T^g_3) = 0$	
Permeation side	$-F_3\frac{dy^g_{i,3}}{dz} + \beta J_{H_2} = 0$	(16)
	$-F_3 C^g_{p_3}\frac{dT^g_3}{dz} + \beta J_{H_2}\int_{T_2}^{T_3} C_p dT + \pi D_i U_{2-3}(T^g_2 - T^g_3) = 0$	(17)
Hydrogen permeation in Pd/Ag membrane	$J_{H_2} = \frac{2\pi L \bar{P}_0}{\ln(\frac{D_o}{D_i})}\exp(\frac{-E_p}{RT})(\sqrt{P_{H_2,2}} - \sqrt{P_{H_2,3}})$	(18)
Boundary conditions	$z = 0, y^g_{i,j} = y^g_{i0,j}, T^g = T^g_0, P^g = P^g_0$	(19)

4.2. Auxiliary correlations

Auxiliary correlations should be added to solve the set of differential equations. The correlations are used to estimate the heat and mass transfer coefficients between two phases, physical properties of chemical species and overall heat transfer coefficient between two sides. These equations are summarized in Table 5. All of the equations solved simultaneously, using Ode (ordinary differential equation) toolbox of MATLAB programming software based on an explicit Runge–Kutta (4,5) formula the Dormand–Prince pair. The reactor is divided into about 500 separate sections.

Table 5 Physical properties, mass and heat transfer correlations.

Parameter	Equation	Reference
Component heat capacity	$C_p = a + bT + cT^2 + dT^{-2}$	[46]
Viscosity	$\mu = \frac{C_1 T^{C_2}}{1 + \frac{C_3}{T} + \frac{C_4}{T^2}}$	[47]
Thermal conductivity	Based on the Chung *et al.* method	[48]
Mass transfer coefficient between gas and solid phases	$k_{gi} = 1.17\,\mathrm{Re}^{-0.42} Sc_i^{-0.67} u_g \times 10^3$ $\mathrm{Re} = \frac{2R_p u_g}{\mu}$ $Sc_i = \frac{\mu}{\rho D_{im} \times 10^{-4}}$	[49]

Parameter	Equation	Reference
	$D_{im} = \frac{1-y_i}{\sum_{i=j} \frac{y_i}{D_{ij}}}$	[50]
	$D_{ij} = \frac{1.43\times10^{-7} T^{3/2} \sqrt{1/M_i + 1/M_j}}{P(v_i^{1/3} + v_j^{1/3})^2}$	[48]
Overall heat transfer coefficient	$\frac{1}{U} = \frac{1}{h_i} + \frac{A_i \ln(D_o/D_i)}{2\pi L K_w} + \frac{A_i}{A_o}\frac{1}{h_o}$	
Heat transfer coefficient between gas phase and reactor wall	$\frac{h}{C_p \rho \mu}\left(\frac{C_p \mu}{K}\right)^{2/3} = \frac{0.458}{\varepsilon_B}\left(\frac{\rho u d_p}{\mu}\right)^{-0.407}$	[51]
Effectiveness factor for reaction k (pore diffusion resistance)	$\eta_k = \frac{\int_0^{R_p} r_k dr}{R_p r_k^s}$	[45]

5. Model validation

Model validation is carried out by comparison of model results and the RIPI pilot plant data, under the design specifications and input data. Table 6 compares the predicted results against experimental data. The selectivity which used here is defined as;

Selectivity = (weight of product) / (normal volume of (CO + H_2) at reactor entrance).

Table 6. Comparison between simulation and plant data for conventional Fischer–Tropsch synthesis reactor.

Parameter	Pilot Plant	Model	Relative Error (%)
X_{H2} (%)	92.83	94.87	2.19
X_{CO} (%)	77.94	74.35	-4.60
C_5^+ Selectivity(g/Nm^3(CO+H_2))	42.55	45.97	8.03
CO_2 Selectivity(g/Nm^3(CO+H_2))	339.07	355.5	4.84
CH_4 Selectivity(g/Nm^3(CO+H_2))	44.15	38.23	-13.42
H_2O Selectivity(g/Nm^3(CO+H_2))	120.67	103.46	-14.26
C_2H_4 Selectivity(g/Nm^3(CO+H_2))	3.95	3.96	0.25
C_2H_6 Selectivity(g/Nm^3(CO+H_2))	11.78	15.18	28.86
C_3H_8 Selectivity(g/Nm^3(CO+H_2))	11.07	9.05	-18.24
n-C_4 Selectivity(g/Nm^3(CO+H_2))	14.45	15.74	8.92
i-C_4 Selectivity(g/Nm^3(CO+H_2))	9.33	11.54	23.68

The calculated results do not deviate from the experimental data significantly.

Simulation results of thermally coupled membrane and non–membrane reactors (TCRs) are compared with the RIPI data for co–current regime. The characteristics for inlet stream of exothermic, endothermic and permeation sections are tabulated in Table 7. The effects of some key operational parameters are considered on gasoline (C_5^+) and hydrogen yields. Below definitions are introduced to examine the reactor performance.

$$\text{Gasoline yield} = \frac{m_{C_{5+}}}{m_{Co} + m_{H_2}} \times 100\% \quad (20)$$

$$\text{Hydrogen recovery yield} = \frac{F_{H_2,3}}{F_{C_6H_{12},in}} \quad (21)$$

Table 7 Operating conditions for Fischer–Tropsch synthesis process (exothermic side), dehydrogenation of cyclohexane to benzene (endothermic side) and permeation side.

Parameter	Value
Exothermic side, Feed composition (mole fraction)	
N_2	0.01
CH_4	0.025
H_2	0.4
H_2O	0.01
CO	0.41
CO_2	0.08
C_2H_4	0.01
C_2H_6	0.014
C_3H_8	0.012
i–C4	0.01
n–C4	0.01
C_5^+	0.02
Endothermic side, Feed composition (mole fraction)	
C_6H_{12}	0.2
C_6H_6	0.001
H_2	0.001
Ar	0.798
Inlet pressure [a] (Pa)	1.013×10^5
Inlet temperature (K)	500
Particle diameter [b] (m)	3.55×10^{-3}
Bed void fraction	0.39
Shell inner diameter (m)	6×10^{-2}
Permeation side, Feed composition (mole fraction)	
Ar (sweep gas)	1.0
H_2	0.0
Total molar flow rate (mol s^{-1})	1.0
Inlet temperature (K)	500
Inlet pressure (Pa)	0.1×10^5
Membrane thickness (m)	6×10^{-6}
Thermal conductivity of membrane (Wm^{-1} K^{-1})	153.95
Shell inner diameter (m)	8×10^{-2}

[a] *Obtained from Jeong et al.* [44]., [b] *Obtained from Koukou et al.* [52].

6. Results and discussions

6.1. Mole balance behavior

Fig. 3(a)–(b) illustrates hydrogen and carbon monoxide conversions for CR and TCRs. A considerable conversion of hydrogen can be achieved in TCRs due to lower temperature and a better heat removal from exothermic side compared with the CR. low temperature shifts the reactions in TCRs toward higher products, especially gasoline, and hence higher conversion of hydrogen.

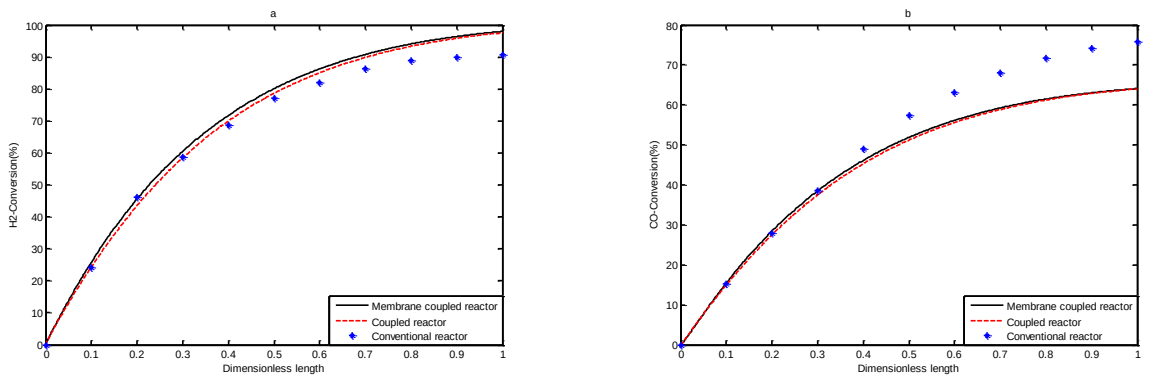

Fig. 3 Comparison of (a) H_2, (b) CO conversion along the reactor axis in exothermic side of membrane, non–membrane coupled reactors with pilot plant data.

Fig. 4(a)–(g) compares hydrocarbon products such as methane, ethylene, ethane, propane, normal–butane, i–butane and gasoline production yields, respectively. Increasing temperature tends to higher reaction rate, highly methane production as an undesirable product. Ji *et al*. [53] showed that high temperature leads to higher light alkanes, alkenes and lower heavy ones. The results show that the new configuration can solve the related issue in the CR and reduces the methane content (Fig. 4(a)). At the same time, the gasoline yield increases as a valuable product. Fig. 4(h) shows CO_2 yield along the reactor. The TCRs operate properly in contrast with the CR, owing to decrease the production of carbon dioxide and its greenhouse effect. Lower temperature in the exothermic side affects water gas shift reaction in favor of CO_2 consumption. A comparison of hydrocarbon products selectivity between TCRs and CR is presented by Fig. 4(i). TCRs enhance the C_5^+ selectivity which is one of the objects of the proposed designs and decline methane selectivity. The coupled configuration is capable to use membrane technology (TCMR) for pure hydrogen production.

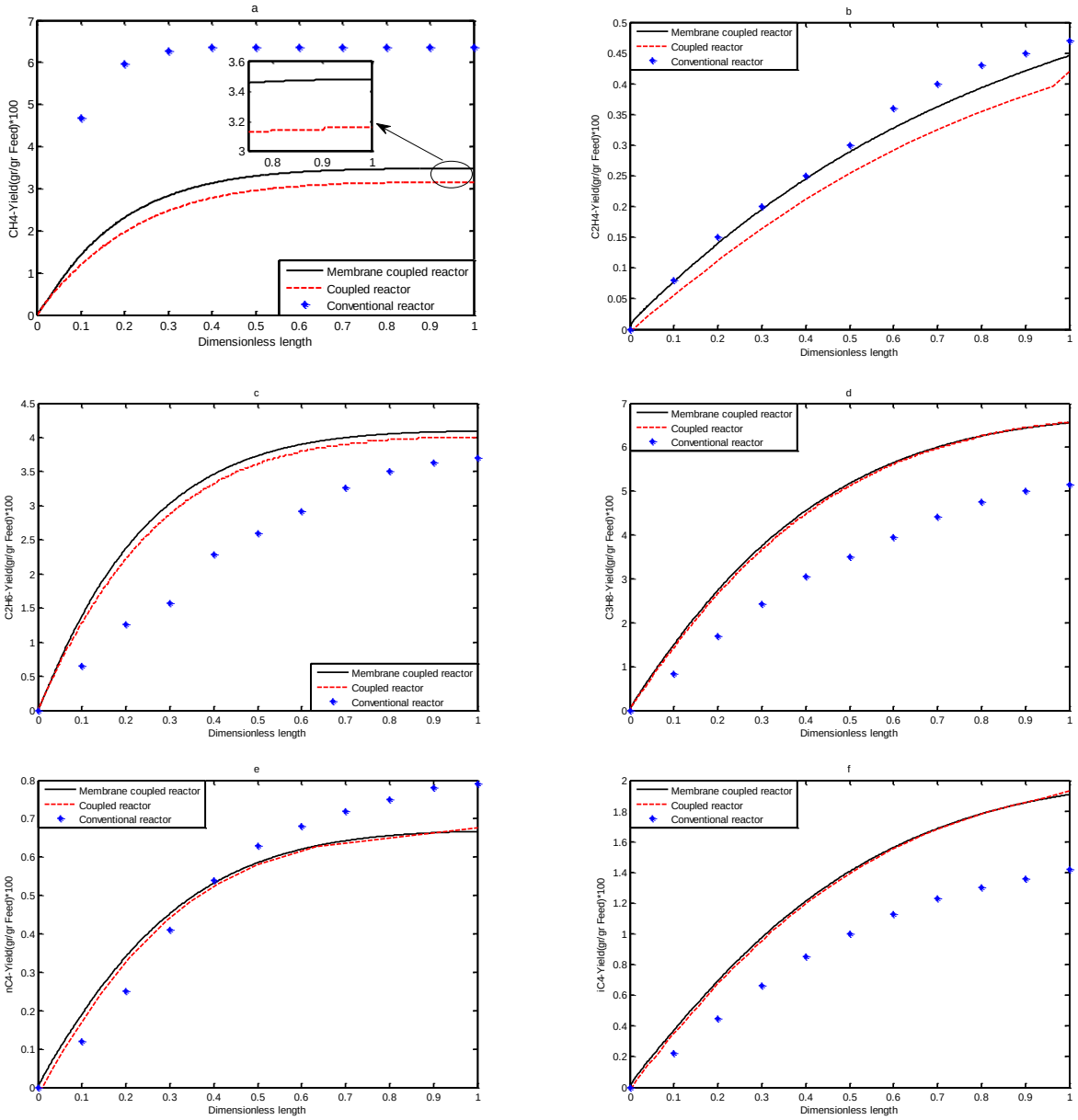

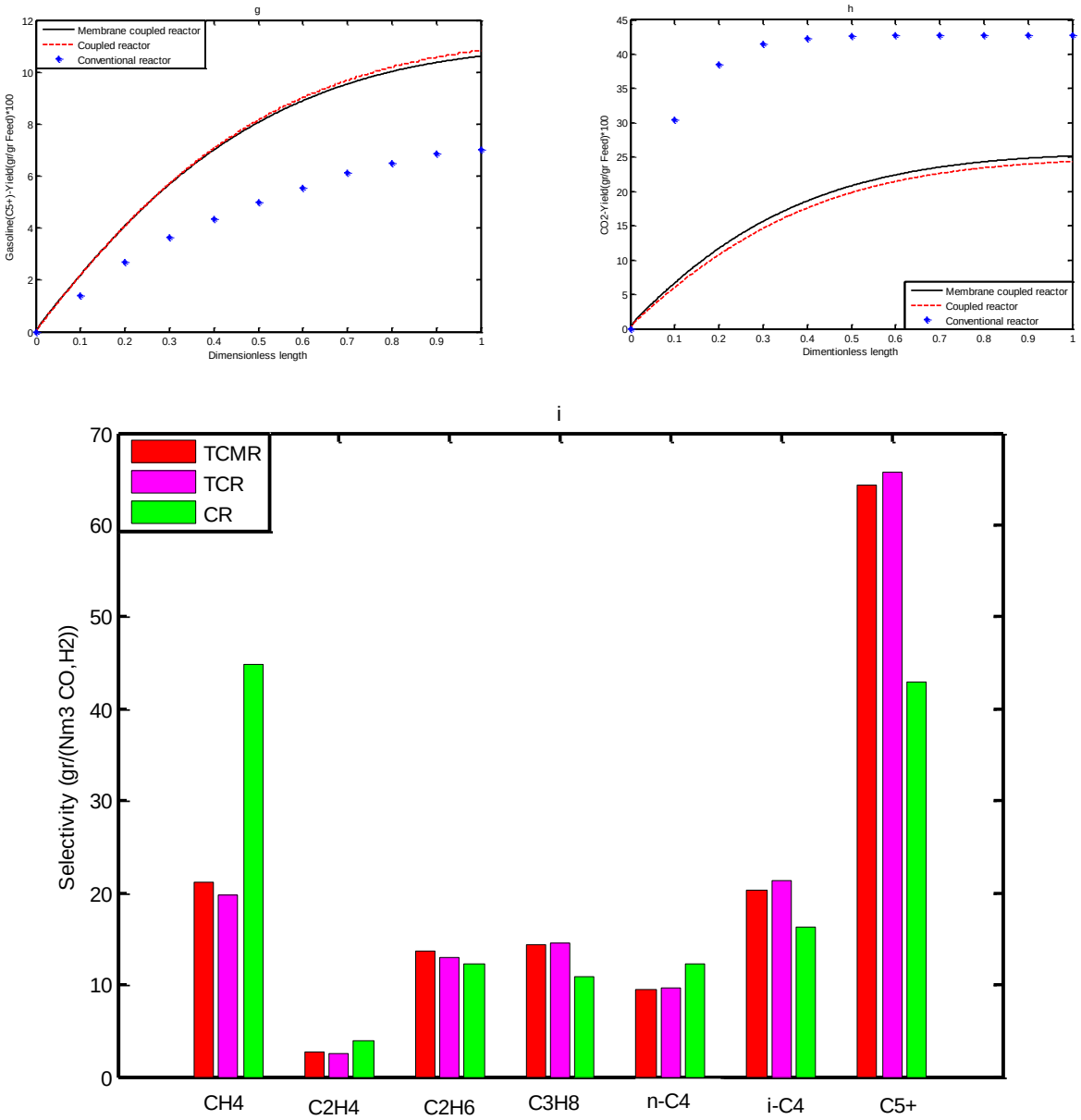

Fig. 4 Comparison of (a) CH_4, (b) C_2H_4, (c) C_2H_6, (d) C_3H_6, (e) n–C_4, (f) i–C_4, (g) C_5^+ and (h) CO_2 yield along the reactor axis in exothermic side of membrane and non–membrane coupled reactors with pilot plant data and (i) Selectivity comparison of the components for the three types of reactor systems.

Fig. 5(a)–(c) shows simultaneous graphs of mole fractions for cyclohexane, benzene and hydrogen in the endothermic side of TCRs vs. dimensionless length. A high percent of chemical reactions are limited by equilibrium. The equilibrium results the reaction would be stopped or reversed. To avoid this, one interesting idea is removal of products from reaction medium (using membrane technology). In other words, in addition to heat transfer, mass (H_2) is transferred via a membrane (Pd-Ag membrane) TCMR. The effective presence of membrane is clearly defined from Fig.5 (c). At the end part of the TCMR the rate of benzene production decreases. This is the consequence of fuel depletion which affects the rate of reaction. The rate of benzene production along the reactor is almost constant due to higher cyclohexane concentration in TCR compared with the TCMR. Also the reactor length is relatively long which yields the same concentrations of benzene and cyclohexane at the outlet of TCRs (Figs. 5(a) and (b)). Hydrogen recovery of membrane reactor is about 1.94.

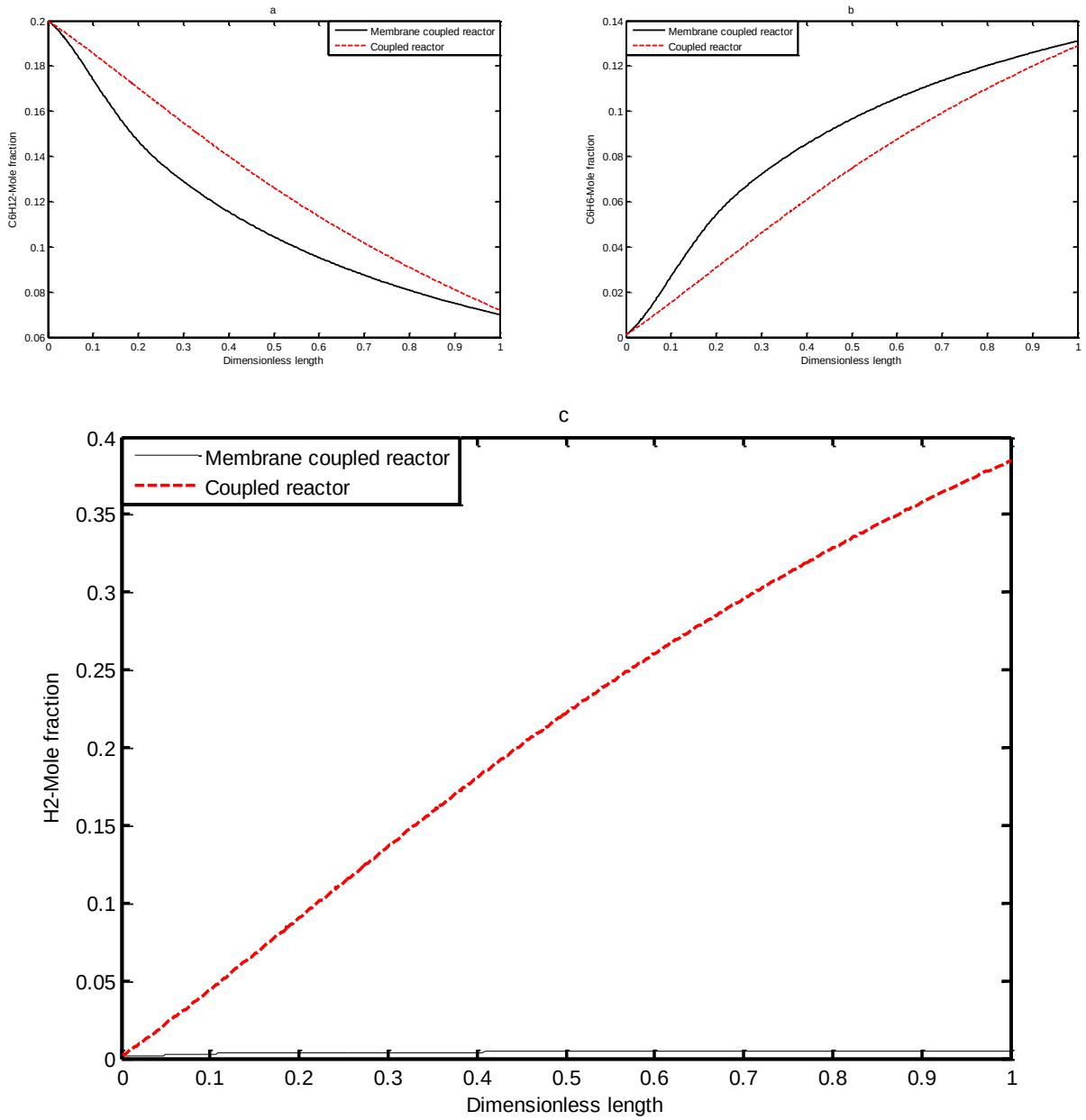

Fig. 5 Profiles of (a) cyclohexane, (b) benzene and (c) hydrogen mole fraction along the reactor axis in the endothermic side of membrane and non–membrane reactors.

6.2. Thermal behavior

Fig. 6(a) shows the temperature gradients in three sides of TCMR, respectively. Heat transfer from exothermic side increases dehydrogenation rate in the reactor entrance (dimensionless length= 0– 0.3). Increasing in temperature is not appreciable because of high flow rate of endothermic side. After dimensionless length= 0.3 the heat transfer direction will reverse and both sweeping and exothermic sides supply the required heat to drive the endothermic reaction (Fig. 6(a)). Fig. 6(b)–(d) reveals temperature profiles in three sides of TCRs. TCR has lower temperature due to elimination of sweeping side as a heat source (Fig.6 (b)–(c)). A jumped temperature can be observed in the CR thermal profile [30] which increases the risk of temperature runaway and makes alert for catalyst deactivation. Fig. 6(b) illustrates the superiority of TCRs to keep the catalyst safe from sintering and deactivation. Fig. 6(d) describes the temperature profile of permeation side.

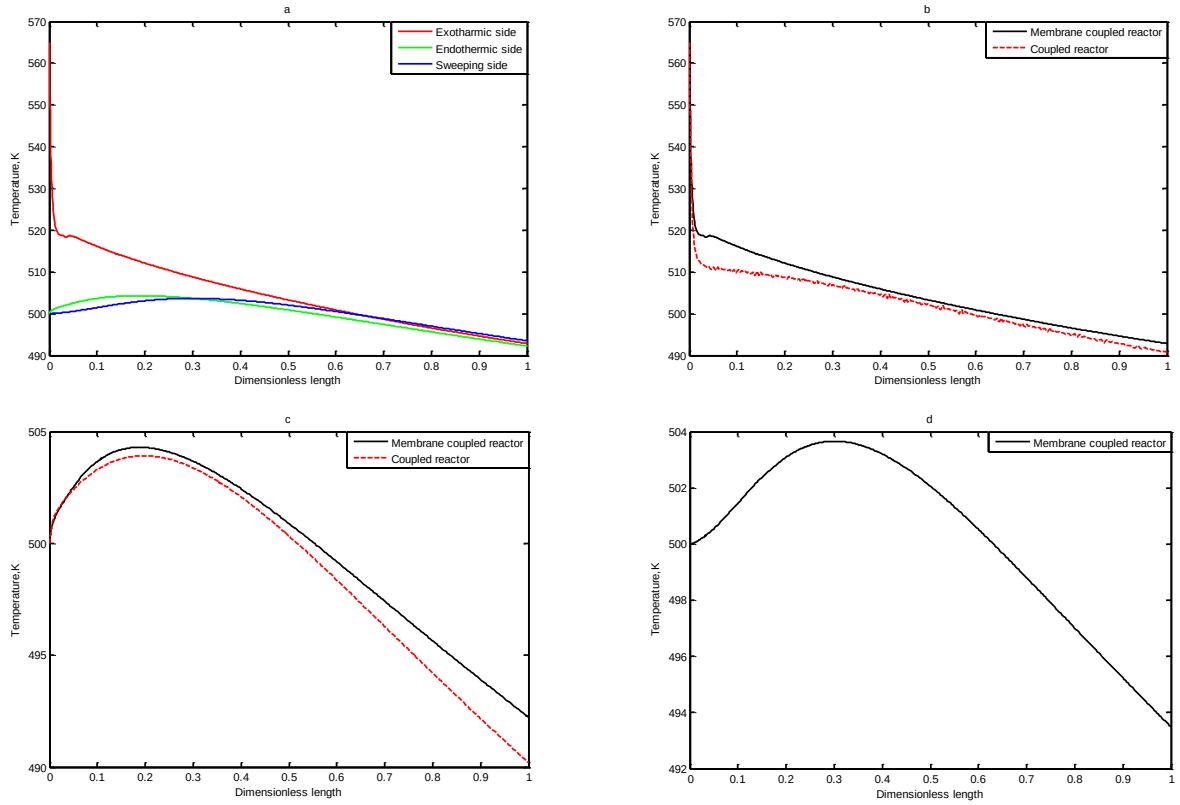

Fig. 6 Comparison of temperature profiles in three sides of thermally coupled membrane reactor (a), variation of temperature for membrane and non–membrane thermally coupled reactors in (b) exothermic side, (c) endothermic side and (d) permeation (sweeping) side along the reactor axis.

6.3. Influence of molar flow rate of endothermic stream

Fig. 7(a) illustrates the variation of gasoline yield and cyclohexane conversion vs. endothermic molar flow rate up to 2 mol s^{-1}. Cyclohexane conversion significantly decreases from 99.83% to 3.28%. Gasoline yield increases as the molar flow rate increases. Gasoline yield increases from 10.37 to 11.07. Cyclohexane conversion decreases as a result of reducing the residence time on the catalyst surface. As Fig. 7(b) shows, increasing in molar flow rate of endothermic stream results in reduction of hydrogen recovery yield from 1.98 to 0.04.

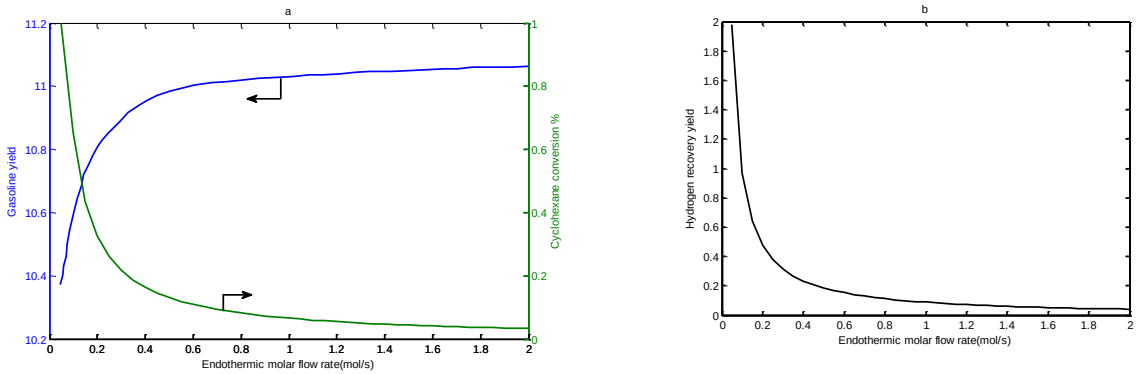

Fig. 7 Influence of molar flow rate of endothermic stream on (a) gasoline yield and cyclohexane conversion and (b) hydrogen recovery yield.

6.4. Influence of membrane thickness

To enhance the hydrogen recovery yield in TCMR, thickness of the membrane should be reduced. Pd–based membranes have a high selectivity for hydrogen but the rate of hydrogen permeation in Pd membrane is low. To overcome this problem many efforts have been made

to reduce the thickness of the Pd–based membrane reactor by producing a thin layer of palladium on a support like alumina and stainless steel. Larger pores and the high selectivity of the Pd–based membrane to hydrogen make it possible to obtain both high permeability and selectivity [15]. Fig. 8 demonstrates the effect of membrane thickness on the hydrogen recovery yield. The reduction of membrane thickness from 50 μm to 6 μm can enhance hydrogen recovery yield. The cyclohexane conversion and gasoline yield do not change significantly by using a thicker membrane.

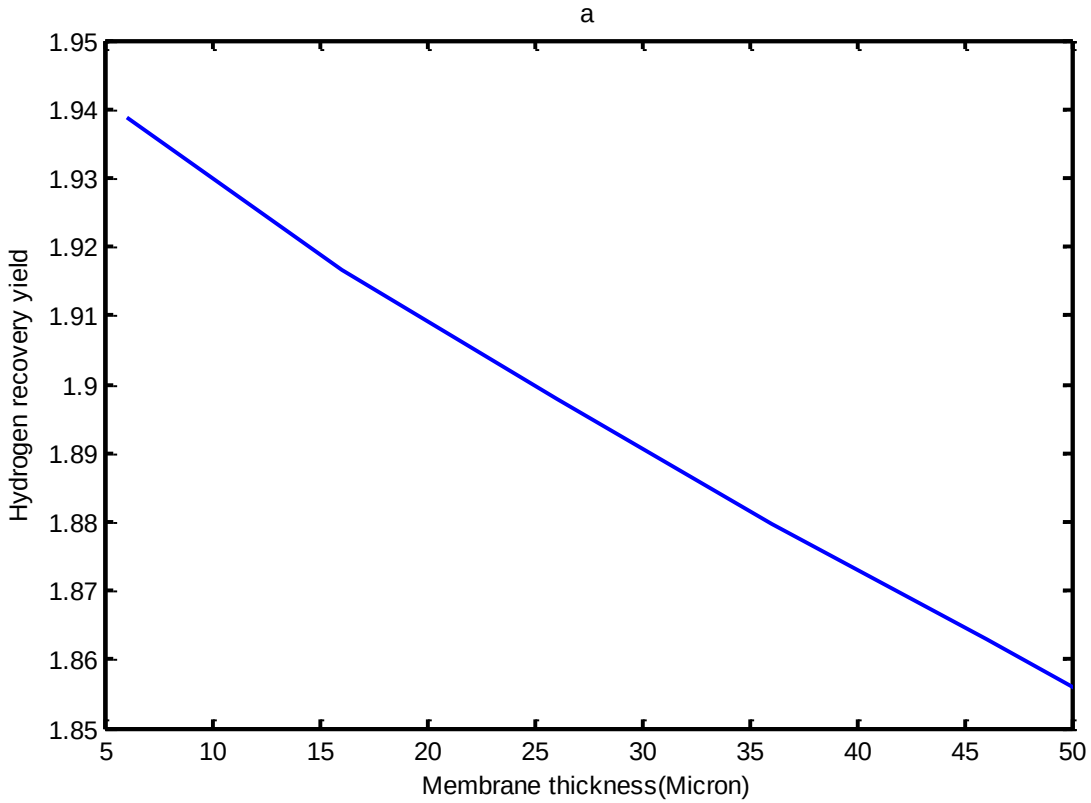

Fig. 8 Influence of membrane thickness on hydrogen recovery yield.

6.5. Influence of molar flow rate of exothermic stream

The effect of changing in exothermic molar flow rate is checked by Figs. 9(a) and (b). Increasing the exothermic molar flow rate decreases significantly the gasoline yield from 11.08 to 7.43 which is due to lower residence time. Cyclohexane conversion and hydrogen recovery yield increase to 99.61% and 2.95, respectively.

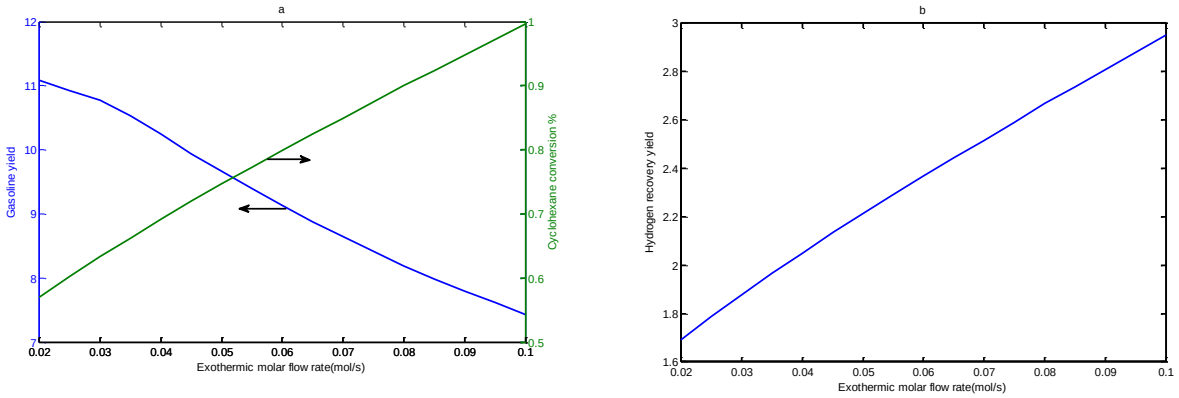

Fig. 9 Influence of molar flow rate of exothermic stream on (a) gasoline yield and cyclohexane conversion and (b) hydrogen recovery yield.

7. Conclusion

The performance of the conventional FT reactor was enhanced by substituting the industrial reactor with the thermally coupled recuperative reactor. The dehydrogenation of cyclohexane occurred in the shell side of RIPI pilot plant. The possibility of using membrane technology was investigated to produce pure hydrogen in TCMR.

This configuration represents some important improvements compared to conventional Fischer-Tropsch processes as follow: direct heat transfer and short distance between heat source and sink increase the thermal efficiency of reactor; using membrane for hydrogen production makes the plant more compact and reduces the size of utilities; pure hydrogen produces (about 2.4 ton/year) for different use especially in fuel cell technology; increasing in gasoline yield and reducing in undesirable products such as methane and carbon dioxide compare with the pilot plant. Because of the complexity of the process involved and because of the interaction of exothermic and endothermic reactions in heat exchanger reactors, a suitable mathematical model is required for the optimization of the process and for reactor control. The results indicate that autothermality can be achieved in TCRs for F–T synthesis reaction and cyclohexane dehydrogenation if the flow rates, inlet temperatures and membrane thickness are properly designed.

Acknowledgment

The authors would like to thank Iranian Oil and Gas Co. and also South Zagross Gas and Oil Company for financial supports. Also cooperation of Mr. Ehsan Pourazadi and Mr. Payam Setudeh for his beneficial suggestions on this work is appreciated.

Nomenclature

a_v Specific surface area of catalyst pellet ($m^2\ m^{-3}$)
A_c Cross section area of each tube (m^2)
A_i Inside area of inner tube (m^2)
A_o Outside area of inner tube (m^2)
C Total concentration (mol m^{-3})
C_p Specific heat of the gas at constant pressure (J mol^{-1})
d_p Particle diameter (m)
D_i Tube inside diameter (m)
D_{ij} Binary diffusion coefficient of component i in j ($m^2\ s^{-1}$)
D_{im} Diffusion coefficient of component i in the mixture ($m^2\ s^{-1}$)
D_o Tube outside diameter (m)
D_{sh} Shell inside diameter (m)
E_i Activation energy(Jmol^{-1})
F Total molar flow rate (mol s^{-1})
h_f Gas–solid heat transfer coefficient (W $m^{-2}\ K^{-1}$)
h_i Heat transfer coefficient between fluid phase and reactor wall in exothermic side (W $m^{-2}\ K^{-1}$)
h_o Heat transfer coefficient between fluid phase and reactor wall in endothermic side (W $m^{-2}\ K^{-1}$)
$\Delta H_{f,i}$ Enthalpy of formation of component i (J mol^{-1})
K Rate constant of dehydrogenation reaction (mol $m^{-3}\ Pa^{-1}\ s^{-1}$)
k_i Rate constant for the i^{th} rate equation of Fischer–Tropsch synthesis reaction
k_{gi} Mass transfer coefficient for component i (m s^{-1})
K Conductivity of fluid phase (W $m^{-1}\ K^{-1}$)
K_B Adsorption equilibrium constant for Benzene (Pa^{-1})
K_p Equilibrium constant for dehydrogenation reaction (Pa^3)
K_w Thermal conductivity of reactor wall (W $m^{-1}\ K^{-1}$)
L Reactor length (m)
M_i Molecular weight of component i (gr mol^{-1})
N Number of components (N = 12 for Fischer Tropsch synthesis reaction, N = 4 for dehydrogenation reaction)
P Total pressure (for exothermic side: bar; for endothermic side: Pa)

P_i Partial pressure of component *i* (Pa)
r_c Rate of reaction for dehydrogenation of Cyclohexane (mol m^{-3} s^{-1})
r_i Reaction rate of component *i* (for exothermic reaction: mol kg^{-1} s^{-1}; for endothermic reaction: mol m^{-3} s^{-1})
R Universal gas constant (J mol^{-1} K^{-1})
R_p Particle radius (m)
Re Reynolds number
Sc_i Schmidt number of component *i*
T Temperature (K)
U Superficial velocity of fluid phase (m s^{-1})
u_g Linear velocity of fluid phase (m s^{-1})
U Overall heat transfer coefficient between exothermic and endothermic sides (W m^{-2} K^{-1})
v_i Atomic Diffusion Volumes
y_i Mole fraction of component *i* (mol mol^{-1})
Z Axial reactor coordinate (m)

Greek letters

M Viscosity of fluid phase (kg m^{-1} s^{-1})
H Effectiveness factor
P Density of fluid phase (kg m^{-3})
ρ_b Density of catalytic bed (kg m^{-3})
T Tortuosity of catalyst

Superscripts

G In bulk gas phase S At surface catalyst

Subscripts

0 Inlet conditions
B Benzene
C Cyclohexane
I Chemical species
J Reactor side (1: exothermic side, 2: endothermic side)
K Reaction number index

References

[1] Huang, X.: Supercritical Fluids as Alternative Media for Fischer-Tropsch Synthesis, Auburn University, Doctor of Philosophy Thesis, August 2003.
[2] Khakdaman, H. R. , Sadaghiani, K.: Separation of Catalyst Particles and Wax From Effluent of a Fischer Tropsch Slurry Reactor Using Supercritical Hexane, IChemE 85 (A2) 263–268.
[3] Ji, Y. Y., Xiang, L. W., Yang, H. J., Xu, Y. Y., Li, Y. W., Zhong, B.: Effect of reaction conditions on the product distribution during Fischer–Tropsch synthesis over an industrial Fe-Mn catalyst, Appl. Catal A: General 214, 77–86 (2001).
[4] Huang, X., Elbashir, N. O., Roberts, C. B.: Supercritical Solvent Effects on Hydrocarbon Product Distributions from Fischer-Tropsch Synthesis over an Alumina-Supported Cobalt Catalyst, Ind. Eng. Chem. Res 43, 6369-6381 (2004).
[5] Pregger, T., Graf, D. , Krewitt, W., Sattler, C., Roeb, M., Moller, S.: Prospects of solar thermal hydrogen production processes, Int. J. Hydrog. Energy 34, 4256–4267 (2009).
[6] Song, C.: Fuel processing for low–temperature and high temperature fuel cells: challenges, and opportunities for sustainable development in the 21st century, Catal. Today 177, 17–49 (2002).
[7] Rahimpour, M.R., Asgari, A.: Production of hydrogen from purge gases of ammonia plants in a catalytic hydrogen–perm selective membrane reactor, Int. J. Hydrog. Energy 34, 5795–5802 (2009).
[8] Brawn, LF.: A comparative study of fuel for on–board hydrogen production for fuel cell powered automobiles, Int. J. Hydrog. Energy 26, 381–97 (2001).

[9] Freni, S., Mondello, N., Cavallaro, S., Cacciola, G., Pardon, V.N., Sobyanin, V.A.: Hydrogen production by steam reforming of ethanol: a two process, React. Kinet. Catal. Lett. 177, 143–52 (2000).
[10] Wiese, W., Emonts, B., Peters, R.: Methanol steam reforming in a fuel cell drive system, J. Power. Sources 84, 187–93 (1999).
[11] Manzolini, G., Tosti, S.: Hydrogen production from ethanol steam reforming: energy efficiency analysis of traditional and membrane processes, Int. J. Hydrog. Energy 33, 5571– 82 (2008).
[12] Breen, J.P., Burch, R., Coleman, H.M.: Metal– catalyzed steam reforming of ethanol in the production of hydrogen for fuel cell applications, App. Catal. 39, 65–74 (2002).
[13] Simbeck, D.R.: Hydrogen costs with CO_2 capture, 7th international conference on greenhouse gas control technologies, Canada, 2004.
[14] U.S. Department of Energy/Morgantown Energy Technology Center. Program research and development announcement for: advanced concepts in ceramic membranes for high temperature gas separation, RFP No. DE–RA21–89MC26038; December, 1988.
[15] Khademi, M.H., Jahanmiri, A., Rahimpour, M.R.: A novel configuration for hydrogen production from coupling of methanol and Benzene synthesis in a hydrogen perm selective membrane reactor, Int. J. Hydrog. Energy 34, 5091–5107 (2009).
[16] Itoh, N., Tamura, E., Hara, S., Takahashi, T., Shono, A., Satoh, K., Namba, T.: Hydrogen recovery from Cyclohexane as a chemical hydrogen carrier using a palladium membrane reactor, Catal. Today 82, 119–125 (2003).
[17] Baker, R.: Future directions of membrane gas-separation technology, Membrane Technology and Research Incorporated, Menlo park, California, USA.
[18] Rahimpour, M.R., ElekaeiBehjati, H.: Dynamic optimization of membrane dual–type methanol reactor in the presence of catalyst deactivation using genetic algorithm, Fuel Process. Technol. 90, 279–291 (2009).
[19] Rahimpour, M.R., Elekaei, H.: Enhancement of methanol production in a novel fluidized–bed hydrogen– perm selective membrane reactor in the presence of catalyst deactivation, Int. J. Hydrog. Energy 34, 2208–2223 (2009).
[20] Rahimpour, M.R.: Enhancement of hydrogen production in a novel fluidized–bed membrane reactor for naphtha reforming, Int. J. Hydrog. Energy 34, 2235–2251 (2009).
[21] KhosravanipourMostafazadeh, A., Rahimpour, M.R.: A membrane catalytic bed concept for naphtha reforming in the presence of catalyst deactivation, Chem. Eng. Process. 48, 683–694 (2009).
[22] Rahimpour, M.R., Elekaei, H.: Optimization of a novel combination of fixed and fluidized–bed hydrogen– perm selective membrane reactors for Fischer–Tropsch synthesis in GTL technology, Chem. Eng. J. 152, 543–555 (2009).
[23] Forghani, A.A., Elekaei, H., Rahimpour, M.R.: Enhancement of gasoline production in a novel hydrogen perm selective membrane reactor in Fischer–Tropsch synthesis of GTL technology, Int. J. Hydrog. Energy 34, 3965–3976 (2009).
[24] Rahimpour, M.R., KhosravanipourMostafazadeh, A., Barmaki, M.M.: Application of hydrogen–perm selective Pd–based membrane in an industrial single–type methanol reactor in the presence of catalyst deactivation, Fuel Process. Technol. 89, 1396–1408 (2008).
[25] Rahimpour, M.R., Elekaei, H.: A comparative study of combination of Fischer–Tropsch synthesis reactors with hydrogen–perm selective membrane in GTL technology, Fuel Process. Technol. 90, 747–761 (2009).
[26] Tosti, S., Basile, A., Bettinali, L., Borgognoni, F., Gallucci, F., Rizzello, C.: Design and process study of Pd membrane reactors, Int. J. Hydrog. Energy 33, 5098–5105 (2008).
[27] Lin, Y.M., Rei, M.H.: Int. J. Hydrog. Energy 25, 211 (2000).
[28] Nair, B.K.R., Choi, J., Harold, M.P.: Electroless plating and permeation features of Pd and Pd-Ag hollow fiber composite membranes, J. Membr. Sci. 288, 67–84 (2007).
[29] Akhtar, A., Pareek, V.K., Tade, M.O.: Modern trends in CFD simulations: application to GTL technology, Chem. Prod. Process. Model. 1, article 2 (2006).
[30] Marvast, M.A., Sohrabi, M., Zarrinpashneh, S., Baghmisheh, GH.: Fischer–Tropsch synthesis: modeling and performance study for Fe–HZSM5 bifunctional catalyst, Chem. Eng. Technol. 1, 28 (2005).

[31] Zanfir, M., Gavriilidis, A.: Modelling of a catalytic plate reactor for Dehydrogenation-combustion coupling, Chem. Eng. Sci., 56, 2671-2683 (2001).
[32] Wei, Z.: A Review of Techniques for the Process Intensification of Fluidized Bed Reactors, Chin. J. Chem. Eng., 17(4), 688-702 (2009).
[33] Ramaswamy, R. C.: Steady State and Dynamic Reactor Models for Coupling Exothermic and Endothermic Reactions, Washington University, Doctor of Science theses, May 2006.
[34] Ramaswamy, R.C., Ramachandran, P.A., Dudukovi´c, M.P.: Recuperative coupling of exothermic and endothermic reactions, Chem. Eng. Sci. 61, 459–472 (2006).
[35] Hunter, J.B., McGuire, G.,: Method and apparatus for catalytic heat–exchange, US Patent.4,214,867 (1980).
[36] Choudhary, V.R., Mulla, S.A.R., Rane, V.H.: Coupling of exothermic and endothermic reactions in oxidative conversion of ethane to ethylene over alkaline earth promoted La_2O_3 catalysts in presence of limited O_2, Appl. Energy 66, 51–62 (2000).
[37] Itoh, N., Wu, T.H.: An adiabatic type of palladium membrane reactor for coupling endothermic and exothermic reactions, J. Membr. Sci. 124, 213–22 (1997).
[38] Khademi, M.H., Setoodeh, P., Rahimpour, M.R., Jahanmiri, A.: Optimization of methanol synthesis and cyclohexane dehydrogenation in a thermally coupled reactor using differential evolution (DE) method, Int. j. Hydrog. Energy 34, 6930–6944 (2009).
[39] Khademi, M.H., Rahimpour, M.R., Jahanmiri, A.: Differential evolution (DE) strategy for optimization of hydrogen production, cyclohexane dehydrogenation and methanol synthesis in a hydrogen-perm selective membrane thermally coupled reactor, Int. j. Hydrog. Energy 35, 1936–1950 (2010).
[40] Elnashaie., S.S.E.H., Moustafa, T., Alsoudani, T., Elshishini, S.S.: Modeling and basic characteristics of novel integrated dehydrogenation–hydrogenation membrane catalytic reactors, Comput. Chem. Eng. 24, 1293–1300 (2000).
[41] Abo–Ghander, N.S., Grace, J.R., Elnashaie, S.S.E.H., Lim, C.J : Modeling of a novel membrane reactor to integrate dehydrogenation of Ethyl benzene to styrene with hydrogenation of nitro benzene to aniline, Chem. Eng. Sci. 63, 1817– 1826 (2008).
[42] http://en.wikipedia.org/wiki/Fischer%E2%80%93Tropsch_process.
[43] Itoh, N.: A membrane reactor using palladium, AIChE. J. 33, 1576 –8 (1987).
[44] Jeong, B.H., Sotowa, K.I., Kusakabe, K.: Catalytic dehydrogenation of cyclohexane in an FAU–type zeolite membrane reactor, J. Membr. Sci. 224, 151–8 (2003).
[45] Graaf, G.H., Scholtens, H., Stamhuis, E.J., Beenackers, A.A.C.M.: Intra–particle diffusion limitations in low–pressure methanol synthesis, Chem. Eng. Sci. 45, 773–83 (1990).
[46] Smith, J.M., Van ness, H.C., Abbot, M.M.: Introduction to chemical engineering thermo-dynamic, 6th ed., McGraw–Hill,New York, 2001.
[47] Perry, R.H., Green, D.W., Maloney, J.O.: Perry's chemical engineers' handbook, Seventh ed., McGraw-Hill, 1997.
[48] Reid, R.C., Sherwood, T.K., Prausnitz, J.: The Properties of Gases and Liquids, third ed., McGraw–Hill, New York, 1977.
[49] Cussler, E.L.: Diffusion, Mass Transfer in Fluid Systems, Cambridge University Press, 1984.
[50] Wilke, C.R. : Chem. Eng. Progress 45, 218 (1949).
[51] Smith, J.M.: Chemical Engineering Kinetics, McGraw–Hill, New York, 1980.
[52] Koukou, M.K., Chaloulon, G., Papayannakos, N., Markatos, N.C. : Mathematical modeling of the performance of non–isothermal membrane reactors, Int. J. Heat Mass Transfer 40, 2407–2417 (1997).
[53] Ji, Y.Y., Xiang, H.W., Yang, J.L., Xu, Y.Y., Li, Y.W., Zhong, B.: Effect of reaction conditions on the product distribution during Fischer–Tropsch synthesis over an industrial Fe-Mn catalyst, App. Catal. A: General 214, 77–86 (2001).

Corresponding author, Tel.: +98 21 64543196; fax:+98 21 6413969, Email: iranshahi@aut.ac.ir (D. Iranshahi)